Circulation

ORIGINAL RESEARCH ARTICLE

CARDIOKIN1: Computational Assessment of Myocardial Metabolic Capability in Healthy Controls and Patients With Valve Diseases

Nikolaus Berndt, PhD; Johannes Eckstein, PhD; Iwona Wallach, PhD; Sarah Nordmeyer, MD; Marcus Kelm, MD; Marieluise Kirchner, PhD; Leonid Goubergrits, Dr-Ing; Marie Schafstedde, MD; Anja Hennemuth, Dr-Ing; Milena Kraus, PhD; Tilman Grune, PhD; Philipp Mertins, PhD; Titus Kuehne, MD*; Hermann-Georg Holzhütter, PhD*

BACKGROUND: Many heart diseases can result in reduced pumping capacity of the heart muscle. A mismatch between ATP demand and ATP production of cardiomyocytes is one of the possible causes. Assessment of the relation between myocardial ATP production (MV_{ATP}) and cardiac workload is important for better understanding disease development and choice of nutritional or pharmacologic treatment strategies. Because there is no method for measuring MV_{ATP} in vivo, the use of physiology-based metabolic models in conjunction with protein abundance data is an attractive approach.

METHOD: We developed a comprehensive kinetic model of cardiac energy metabolism (CARDIOKIN1) that recapitulates numerous experimental findings on cardiac metabolism obtained with isolated cardiomyocytes, perfused animal hearts, and in vivo studies with humans. We used the model to assess the energy status of the left ventricle of healthy participants and patients with aortic stenosis and mitral valve insufficiency. Maximal enzyme activities were individually scaled by means of protein abundances in left ventricle tissue samples. The energy status of the left ventricle was quantified by the ATP consumption at rest (MV_{ATP}[rest]), at maximal workload (MV_{ATP}[max]), and by the myocardial ATP production reserve, representing the span between MV_{ATP}(rest) and MV_{ATP}(max).

RESULTS: Compared with controls, in both groups of patients, MV_{ATP}(rest) was increased and MV_{ATP}(max) was decreased, resulting in a decreased myocardial ATP production reserve, although all patients had preserved ejection fraction. The variance of the energetic status was high, ranging from decreased to normal values. In both patient groups, the energetic status was tightly associated with mechanic energy demand. A decrease of MV_{ATP}(max) was associated with a decrease of the cardiac output, indicating that cardiac functionality and energetic performance of the ventricle are closely coupled.

CONCLUSIONS: Our analysis suggests that the ATP-producing capacity of the left ventricle of patients with valvular dysfunction is generally diminished and correlates positively with mechanical energy demand and cardiac output. However, large differences exist in the energetic state of the myocardium even in patients with similar clinical or image-based markers of hypertrophy and pump function.

REGISTRATION: URL: https://www.clinicaltrials.gov; Unique identifiers: NCT03172338 and NCT04068740.

Key Words: energy metabolism ■ heart valve diseases ■ mathematical model ■ metabolism ■ proteomics

Correspondence to: Nikolaus Berndt, Charité-Universitätsmedizin Berlin, Charitéplatz 1, 10117 Berlin, Germany. Email nikolaus.berndt@charite.de

*T. Kuehne and H.-G. Holzhütter contributed equally.

Supplemental Material is available at https://www.ahajournals.org/doi/suppl/10.1161/CIRCULATIONAHA.121.055646.

For Sources of Funding and Disclosures, see page 1936–1937.

Clinical Perspective

What Is New?

- We developed CARDIOKIN1, a novel comprehensive molecular-resolved kinetic model of central cardiac metabolism.
- CARDIOKIN1 enables new insights into regulatory principles of cardiac metabolism and allows patient-specific evaluation of metabolic capacities on the basis of proteomics data.
- We applied the method in patients who had significant change in cardiac workload owing to aortic and mitral valve diseases.

What Are the Clinical Implications?

- Common heart valve diseases, such as aortic stenosis and mitral regurgitation, lead to significant impairment in cardiac metabolic capacity.
- Metabolic capacities have a significant correlation with biomechanical measures such as myocardial power and cardiac output but can vary considerably between individual patients, contributing to understanding why some patients develop heart failure over time, whereas others with similar hemodynamic conditions do not.
- Individual metabolic capacities are associated with postoperative outcomes and may be a helpful prognostic marker.

Nonstandard Abbreviations and Acronyms

AS	aortic stenosis
BCAA	branched-chain amino acid
BP	blood pressure
FFA	free fatty acid
HR	heart rate
KB	ketone body
LV	left ventricle
MAPR	myocardial ATP production reserve
MVI	mitral valve insufficiency
MV_{ATP}	myocardial ATP production capacity
MV_{ATP}(max)	myocardial ATP consumption at maximal workload
MV_{ATP}(rest)	myocardial ATP consumption at rest
MVo_2	myocardial oxygen consumption
NYHA	New York Heart Association

In recent years, numerous studies have firmly established metabolic derangement as a cardinal feature of the pathophysiology of heart diseases.[1–5] Although changes in cardiac metabolism are understood to be an underlying component in almost all cardiac myopathies, the potential contribution of myocardial energy metabolism to the reduction of cardiac performance is not fully understood.[6] As early as 1939, Herrmann and Decherd Jr[7] proposed that the failing heart is an energy-starved engine that has run out of fuel. Several decades later, this concept has been reaffirmed,[3] primarily in light of findings that in the failing heart, the gene expression of key proteins involved in cardiac energy metabolism is downregulated (see examples)[8,9] and so is the level of central metabolic enzymes (eg, creatine kinase)[10] and of cardiac energy-rich phosphates (ATP, CrP), as established by ^{31}P magnetic resonance spectroscopy in vivo.[11,12] Although these findings are suggestive for a mismatch between ATP demand and ATP supply, they do not permit assessment of the degree of mismatch.

A common cause of cardiac dysfunction is valvular heart disease. The most frequent types of valve disease are aortic stenosis (AS) and mitral valve insufficiency (MVI), which expose the heart to long-term pressure or volume overload, respectively. Chronic pressure or volume overload trigger cardiac remodeling, leading to specific forms of myocardial hypertrophy. Pressure overload typically results in eccentric myocardial hypertrophy with wall thickness increase, whereas volume overload is dominated by concentric forms with increase of ventricular chamber volumes. Some patients tolerate the overload condition well for years, whereas others quickly change from compensated to decompensated heart failure despite similar cardiac pump function characteristics. Therefore, it is of particular importance in the clinic to be able to predict the risk for transition from compensated to decompensated heart failure as accurately as possible. This would include better knowledge about the metabolic status of the myocardium in heart diseases. Using cardiac magnetic resonance imaging and ^{31}P magnetic resonance spectroscopy, Peterzan et al.[13] addressed whether reduced delivery of ATP from mitochondria to the myosin ATPase by the creatine kinase shuttle may explain why some (but not all) patients with severe AS develop otherwise unexplained reduced left ventricular (LV) ejection fraction. Their data do not provide evidence for a significant difference in the creatine kinase flux of patients with cardiac dysfunction. This finding raises the question whether it is the gradual reduction in the myocardial ATP production capacity (MV_{ATP}) that parallels the deterioration of the LV systolic function that is at issue. The problem with testing this hypothesis is that no method is available to measure the ATP production rate MV_{ATP} in vivo. The aim of this work was to develop a method allowing assessment of the capability of the LV to increase MV_{ATP} in response to an increase in ATP demand.

On the basis of our network reconstruction of the metabolic network of the cardiomyocyte[14] and previous modeling work on metabolic subsystems,[15–18] we established a complex physiology-based mathematical model of the myocardial energy metabolism. The model encompasses all pathways along which the possible energy-

delivering substrates glucose, long-chain fatty acids, ketone bodies (KBs), acetate, and branched-chain amino acids (BCAAs) are used. As in our previous model-based studies on liver metabolism,[19] we used the proteomics-based abundance of metabolic enzymes in cardiac tissue to generate individualized metabolic models of cardiac energy metabolism. Applying this approach to the LV of controls and patients with MVI and AS, we tested the hypothesis that despite overall preserved systolic function, the ATP production capacity of the LV is reduced and correlates positively with mechanic energy demand and cardiac output.

METHODS

The analytic methods (model equations) are available in the Supplemental Materials for other researchers for purposes of replicating the procedure. Patients' proteomics data will not be made available to other researchers.

Patient Characteristics

We investigated 75 human LV myocardial biopsies. Myocardial samples from the LV septum were collected during surgical aortic or mitral valve replacement from 41 patients with AS and 17 patients with MVI. Patient characteristics are described in the Table. For the controls (n = 17), samples were taken from 44 ≥15-year-old donors without cardiac diseases but whose hearts were not used for transplantation. All samples were frozen immediately in liquid nitrogen until further processing.

The study protocol was in agreement with the principles outlined in the Declaration of Helsinki and was approved by the Medical Ethics Review Committee. All patients gave written informed consent before inclusion.

Quantitative Proteomics of Tissue Samples

LV septum biopsies were extracted at time of surgery, frozen directly in liquid nitrogen, and kept at −80°C. For protein extraction, biopsies were lysed in 200 µL lysis buffer (2% SDS, 50 mM ammonium bicarbonate buffer, and EDTA-free protease inhibitor cocktail [Complete; Roche]) and homogenized using FastPrep-24 5G Homogenizer (MP Biomedicals; 10 cycles of 20 seconds with 5-second pause). After heating for 5 minutes at 95°C and 5 freeze–thaw cycles, Benzonase (25 U; Merck) was added for 30 minutes and lysates were clarified by centrifugation at 16 000 *g* for 40 minutes. A total of 100 µg protein per sample was processed further using the SP3 clean-up and digestion protocol as previously described.[20] Briefly, each sample was reduced with 10 mM dithiothreitol (Sigma), followed by alkylation with 40 mM chloroacetamide (Sigma) and quenching with 20 mM dithiothreitol (Sigma). Next, 1 mg beads and acetonitrile (70% final concentration) were added to each sample and after 20 minutes of incubation, bead-bound protein was washed with 70% ethanol and 100% acetonitrile. Then, 2 µg sequence-grade Trypsin (Promega) and 2 µg LysC (Wako) in 50 mM HEPES (pH 8) were added. After overnight incubation at 37°C, peptides were collected, acidified with trifluoroacetic acid, and cleaned up using the StageTips protocol.[21]

Heart Reference Sample for Matching Library

A peptide mix for each experimental group (control, AS, and MVI) was generated by collecting 10 µg peptides from each individual sample belonging to the corresponding group. Equal peptide amounts from each group mixture were combined, fractionated into 96 fractions by basic reversed-phase chromatography (XBridge C18 4.6 mm × 250 mm column [Waters, 3.5 µm bead size]; Agilent 1290 high-performance liquid chromatography instrument; 90 minutes gradient; flow rate 1 mL/min), and pooled into 26 equal interval fractions for further analyses.

Liquid Chromatography With Tandem Mass Spectrometry Analyses

Peptides were separated by reversed-phase chromatography (20 cm column; 75 µm inner diameter, ReproSil-Pur C18-AQ; 1.9 µm, Dr Maisch GmbH) using a 200-minute gradient (flow rate 250 nL/min) on a high-performance liquid chromatography system (ThermoScientific). Measurements were performed on an Orbitrap Fusion (individual samples) or Q Exactive HF-X Orbitrap instrument (reference sample; ThermoScientific) using data-dependent acquisition. Each sample was measured twice and replicates were joined for data analysis. Data were analyzed using MaxQuant (v1.6.2.6) and a decoy human UniProt database (2019-01).[22] Variable modifications of oxidation (M), N-terminal acetylation, deamidation (N, Q), and fixed modification of carbamidomethyl cysteine were selected. The false discovery rate was set to 1% for peptide and protein identification. Unique and razor peptides were considered for quantification. Match between runs and label-free quantification algorithm were applied.

Description of the Mathematical Model (CARDIOKIN1)

For quantification of the metabolic changes caused by the abundance changes of metabolic enzymes, we developed a mathematical model of the cardiac energy metabolism, which comprises all pathways involved in the catabolism of the energy-delivering substrates glucose, lactate, fatty acids, KBs, and BCAAs, as well as the synthesis of endogenous energy stores (glycogen, triacylglycerol; Figure 1). The model also takes into account the short-term regulation of metabolic enzymes and transporters by the hormones insulin and catecholamines and key electrophysiologic processes at the inner mitochondrial membrane including generation of the proton gradient by the respiratory chain, synthesis of ATP by FoF1-ATPase, and membrane transport of various ions.

The time course of model variables (concentration of metabolites and ions) is governed by first-order differential equations. Time variations of small ions are modeled by kinetic equations of the Goldman-Hodgkin-Katz type as used in our previous work.[23] The rate laws for enzymes and membrane transporters were either taken from the literature or constructed on the basis of published experimental data for the mammalian heart. The used rate laws take into account the regulation of enzymes and transporters by reaction substrates and products, allosteric effectors, and reversible phosphorylation as compiled by biochemists during decades of enzymatic research. Supplement S1 contains all kinetic equations and model parameters sorted by individual pathways. For each kinetic parameter value, we indicated the experimental source.

Table. Patient Characteristics

Characteristics and preoperative function measures	AS	MVI	*P* value
Age at surgery, y	68±9	60±14	0.032
BMI	28±4	27±3	0.343
Female sex	23 (56)	6 (35)	0.414
NYHA functional classification, stage I/II/III/IV	5/17/15/1	2/7/6/2	0.593
Systolic blood pressure, mm Hg	140±19	131±16	0.123
Diastolic blood pressure, mm Hg	74±11	75±13	0.675
EDVI, mL/m^2	73±17	108±34	<0.001
ESVI, mL/m^2	30±11	40±14	0.015
EF, %	60±7	62±9	0.048
CI, L/min/m^2	3±1	5±2	<0.001
CO, L/min	6±2	9±4	<0.001
Internal myocardial power	13±7	13±5	1
Myocardial mass (indexed), g/m^2	71±20	67±15	0.484
Mean pressure gradient aortic valve, mm Hg	56±15	4±8	<0.001
Mitral valve insufficiency, none/mild over moderate to severe	41/0/0	0/10/7	<0.001
Aortic valve insufficiency, none/mild over moderate to severe	36/5/0	17/0/0	0.321
Serum creatinine, mg/dL	0.91±0.15	1.0±0.20	0.065
Hypertension	27 (66)	11 (65)	0.826
Dyslipidemia	8 (20)	3 (18)	0.839
Diabetes type 2	7 (17)	2 (12)	0.913
Coronary artery disease	1 (2)	2 (12)	0.419
Atrial fibrillation, paroxysmal	2 (5)	2 (12)	0.709
Atrial fibrillation, permanent	0 (0)	2 (12)	0.149
Medication ACE inhibitor	15 (37)	5 (29)	0.826
Medication β-blocker	20 (49)	10 (59)	0.683
Medication diuretics	12 (29)	5 (29)	0.760

Data are presented as total number (%) in case of categorical values and as mean±SD in case of numeric values. Significance of parameter differences between the 2 patient groups is given as *P* values. ACE indicates angiotensin-converting enzyme; AS, aortic stenosis; BMI, body mass index; CI, cardiac index; CO, cardiac output; EDVI, end-diastolic volume index; EF, ejection fraction; ESVI, end-systolic volume index; MVI, mitral valve insufficiency; and NYHA, New York Heart Association.

Model Calibration for Individual Hearts

Among the kinetic parameters of the enzymatic rate laws (binding constants of ligands, cooperativity indices), only V_{max}, representing the maximal activity of an enzyme/transporter, may vary among individual LVs as the value of this parameter is proportional to the enzyme abundance: $V_{max} = k_{cat} \cdot E$, with k_{cat} being the turnover rate of a single enzyme and E the enzyme concentration. Exploiting this simple relationship, we used the proteomics-derived protein profiles of enzymes and transporters for model calibration by computing the maximal activities (V_{max}) of the enzymes by the relation

$$V_{\max}^{subject} = V_{\max}^{normal} \frac{E^{subject}}{\langle E^{control} \rangle} \quad (1)$$

where $\langle E^{control} \rangle$ is the average protein intensity of the enzyme in the group of control hearts and $E^{subject}$ is the protein concentration of the enzyme in the individual (control or patient). The maximal activities $v_{\max}^{normal}$ of the reference model for the average normal heart were obtained by fitting of the model to experimental data (Table S2). Relation (1) follows from the fact that the maximal enzyme activity is proportional to the abundance of the protein.

Energetic Capacities of Controls and Patients With Valve Diseases

We used the model to compute the specific uptake rates of substrates and the specific ATP production rate at rest, MV_{ATP}(rest), and at maximal ATP workload, MV_{ATP}(max), for the LV of controls (n=17) and patients with MVI (n=17) or AS (n=41). As a third parameter to characterize the capacity of the LV to increase ATP production with increasing workload, we used the span between MV_{ATP}(max) and MV_{ATP}(rest), which we refer to as myocardial ATP production reserve (MAPR = MV_{ATP}[max] − MV_{ATP}[rest]). In the following, we distinguish among specific energy parameters MV_{ATP}(rest), MV_{ATP}(max), and MAPR quantifying the energetic capacity per mass unit of the LV (given in μmol/g/h) and total energy parameters tMV_{ATP}(rest), tMV_{ATP}(max), and tMAPR quantifying the energetic capacity of the LV (given in mmol/h; ie, tMV_{ATP}[rest] = MV_{ATP}[rest] × LV mass/1000).

The computations were performed for a normal postabsorptive state (overnight fast) characterized by the following metabolite and hormone concentrations: glucose 5.8 mM,[24] fatty acids 0.5 mM,[25] lactate 0.8 mM,[24] glutamine 0.5 mM,[26,27] valine 0.2 mM,[26,27] leucine 0.15 mM,[26,27] isosleucine 0.06 mM,[26,27] β-hydroxybutyrate 0.08 mM,[28,29] and acetoacetate 0.04 mM.[30] The concentration of catecholamines at rest was 0.75 nM[31,32] and increased with growing workload (see Supplement S2, including Figures S1–S4).

The myocardial ATP consumption of the stationary resting state, MV_{ATP}(rest), was chosen in a way that the computed myocardial oxygen consumption (MVo_2) was identical with the participant's MVo_2, which we estimated by the 2-factor approximation[33]

$$MV_{O2} = \gamma \cdot HR \cdot BP \quad (2)$$

using heart rate (HR) and peak systolic blood pressure (BP) and γ as a proportionality factor. Resting MVo_2 of normal hearts was found in the range of 0.8 to 1.2 mL/min/g.[2,4,34] Thus, with a mean MVo_2 of 0.1 mL/min/g, HR of 70/min, and normal BP of 125 mm, we set γ to 1.143×10^{-5} mL/mm Hg/g.

The metabolic response of the ventricle to an additional workload (pacing) was evaluated by computing the temporal changes of the metabolic state elicited by an increase of the ATP consumption rate above the resting value. The ATP consumption rate was modeled by a generic hyperbolic rate law

$$v_{ATP} = k_{load} \cdot \frac{ATP}{ATP + K_m} \quad (3)$$

(Supplement S1). The parameter k_{load} was stepwise increased until MV_{ATP} converged to the maximum: MV_{ATP}(max).

To evaluate the mechanical burden of the heart, we calculated the internal myocardial power, which describes the energy required for cardiac contraction for the individual hearts (see methods used in Lee et al[35]).

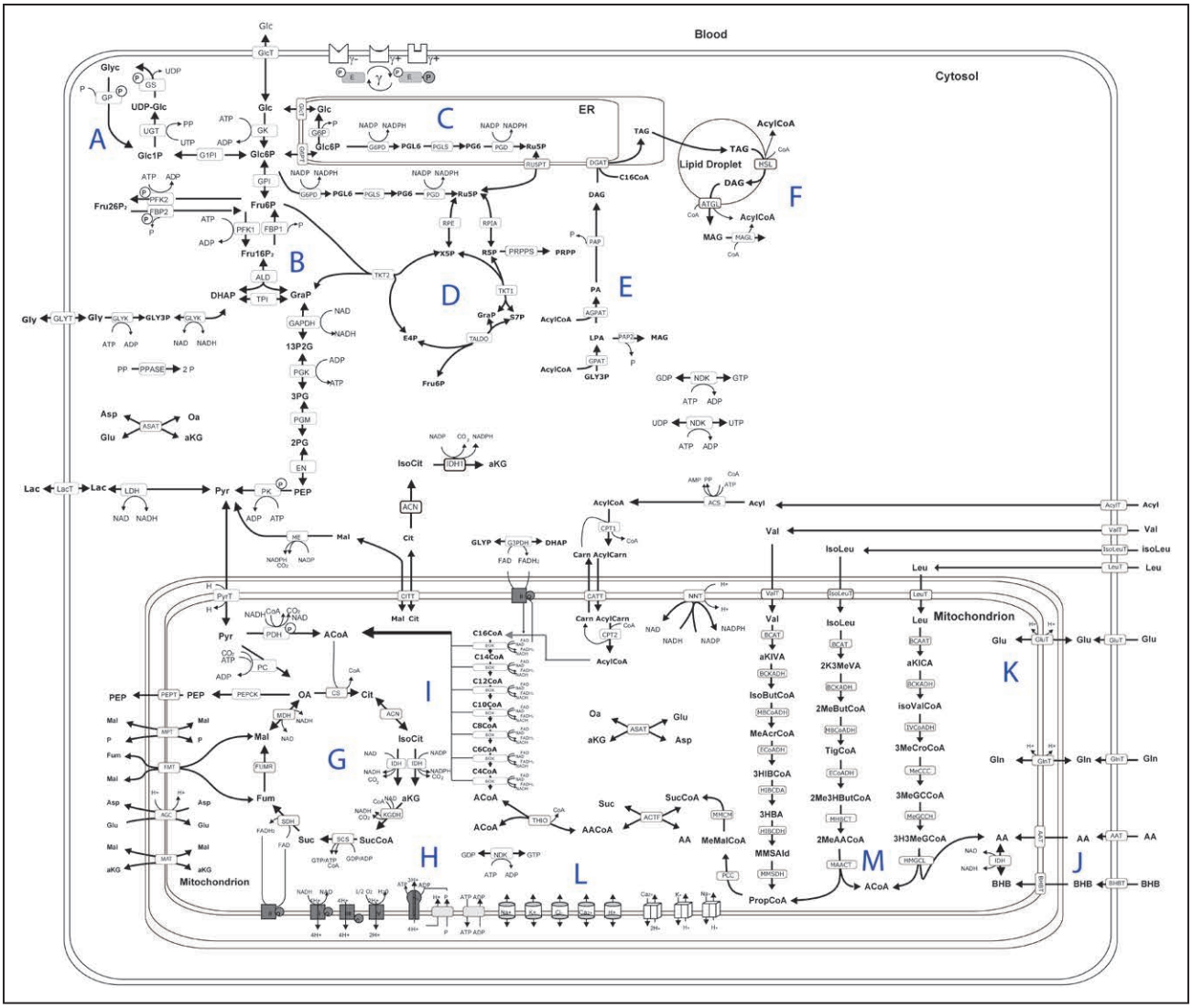

Figure 1. Reaction scheme of the metabolic model.
Arrows symbolize reactions and transport processes between compartments. **A**, Glycogen metabolism, (**B**) glycolysis, (**C**) oxidative pentose phosphate pathway in the endoplasmic reticulum and cytosol, (**D**) nonoxidative pentose phosphate pathway, (**E**) triglyceride synthesis, (**F**) synthesis and degradation of lipid droplets, (**G**) tricarbonic acid cycle, (**H**) respiratory chain and oxidative phosphorylation, (**I**) β-oxidation of fatty acids, (**J**) ketone body utilization, (**K**) glutamate metabolism, (**L**) mitochondrial electrophysiology (membrane transport of ions), and (**M**) utilization of branched-chain amino acids. Small cylinders and cubes symbolize ion channels and ion transporters. Double arrows indicate reversible reactions, which, according to the value of the thermodynamic equilibrium constant and cellular concentrations of their reactants, may proceed in both directions. Reactions are labeled by the short names of the catalyzing enzyme or membrane transporter given in the small boxes attached to the reactions arrow. Metabolites are denoted by their short names. Full names and kinetic rate laws of reaction rates are outlined in Supplement S1. Full names of metabolites and a comparison of experimentally determined and calculated cellular metabolite concentrations are given in Table S1.

All model simulations were performed using MATLAB, Release R2011b (The MathWorks, Inc).

RESULTS

Model Calibration for the Normal Heart

Except for the maximal enzyme activities (V_{max} values), which may vary owing to variable gene expression, the numeric values for all other parameters of the enzymatic rate laws were taken from reported kinetic studies of the isolated enzymes. Numeric values for the V_{max} values (Table S2) were estimated by the same procedure that was used for the calibration of our metabolic liver model[19]: calculated metabolite profiles and fluxes were adjusted to experimental data from independent experiments with perfused hearts and in vivo measurements whereas the metabolite concentrations were constrained to experimentally determined ranges (Table S1). Short-term regulation of key regulatory enzymes by the hormones insulin and catecholamines (epinephrine, norepinephrine) was included into the model by phenomenologic mathematical functions relating the enzyme's phosphorylation state and the abundance of the GLUT4 transporter in the

sarcolemma to the plasma concentrations of glucose (insulin) and the exercise level (catecholamines; Supplement S2). Model simulations, which correctly recapitulate metabolic measurements obtained with perfused hearts and in human in vivo studies, comprise glucose utilization at varying exogenous glucose concentrations; lactate utilization and lactate/O_2 ratio at varying exogenous lactate concentrations; utilization of free fatty acids (FFAs) at varying exogenous FFA concentrations; glucose utilization in response to varying exogenous concentration of FFAs (glucose–FFA competition); KB utilization at varying exogenous β-hydroxybutyrate concentrations; utilization rates of glucose, lactate, FFAs, KBs, and BCAA under postabsorptive resting conditions; and utilization rates of glucose, lactate, FFAs, KBs, and BCAAs at moderate pacing. Details of all validation simulations are given in Supplement S3 (including Figures S5–S10 and Tables S3–S8).

Figure 2 shows 2 model validations highlighting the good concordance of model predictions with experimental data. The examples demonstrate the ability of the heart to ensure cardiac functionality at varying cardiac workloads and varying plasma concentrations of energy substrates. In Figure 2A, the computed substrate uptake profile of the normal human heart is compared with the mean of experimental data taken from several in vivo studies.[36–43] At rest, lactate is utilized with the highest rate, followed by FFAs and KBs. Counted in moles ATP per moles substrate (textbook values: glucose 38, lactate 18, palmitate 138), FFAs represent the dominating energy source. At moderate pacing, the uptake of the carbohydrates is more than doubled, whereas the uptake of FFAs remains essentially unaltered. The energetic contribution of BCAAs was <1% at rest and pacing. Figure 2B shows the relationship between glucose uptake and plasma FFA concentration. The uptake rate of glucose is suppressed with increasing levels of plasma FFAs by inhibition of glucose uptake[44] ensuring the preferential utilization of fatty acids (Figure 2B).

Patient-Specific Model Calibration

For patient-specific model calibration, we used protein intensity profiles (defined through label-free quantification intensities; see Methods) of 17 control hearts, 41 patients with AS, and 17 patients with MVI. Using 2-dimensional liquid chromatography before tandem mass spectrometry analysis, we identified, in total, 9133 distinct protein groups, from which a subset of 321 proteins was used for model calibration.

Energetic Capacities of the LV of Controls and Patients With Valve Diseases

Figure 3 depicts the specific energetic parameters MV_{ATP}(rest), MV_{ATP}(max), and MAPR for each participant after 60-minute pacing. Compared with controls, the individual variations of these parameters were much larger for the 2 patient groups (see box plots in Figure 3B–3D). For patients with MVI, the mean value of the param-

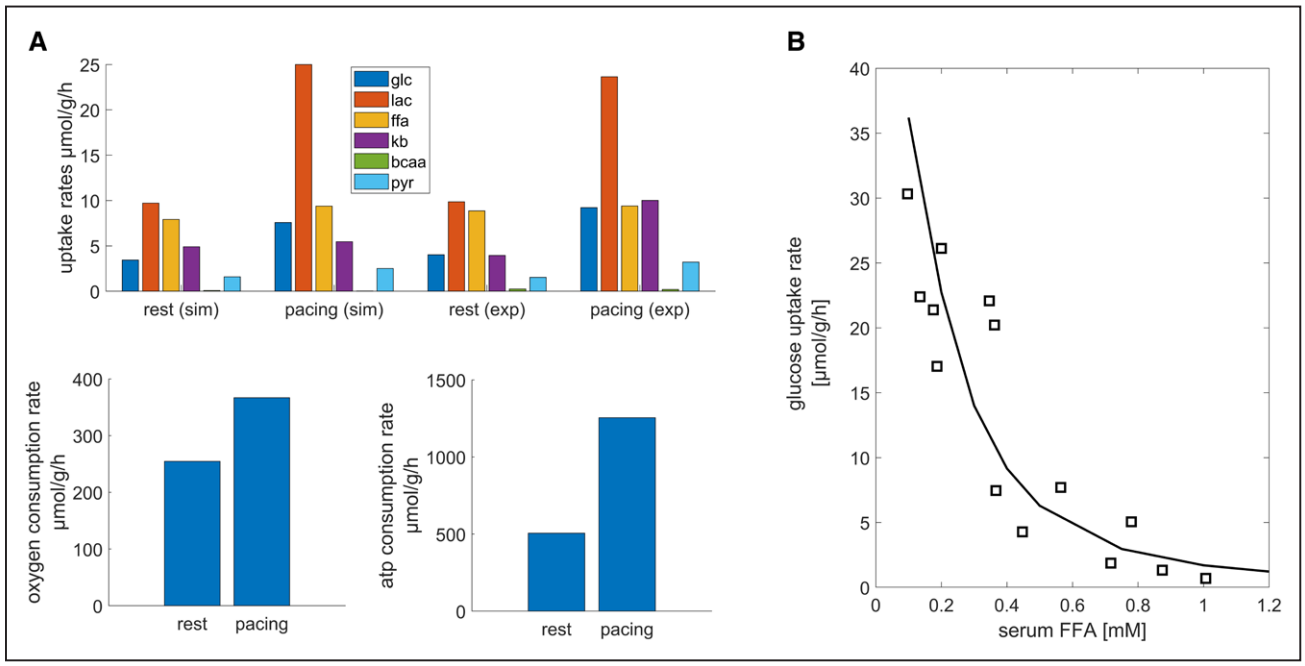

Figure 2. Simulated and measured myocardial substrate uptake rates in vivo.
A, Substrate uptake rates at rest and at moderate pacing (50% maxVo_2). (sim) Uptake rates were computed from reported extraction rates (1 – arterial concentration/concentration in coronary sinus) putting the coronary blood flow to 0.8 mL/min/g and heart weight to 300 grams. (exp) The data points represent the means of various experimental studies.[37,38,40–43,45] **B**, Dependence of the glucose uptake rate from the plasma concentration of free fatty acids (FFAs). The solid line represents model values; squares symbolize in vivo data taken from Nuutila et al.[44]

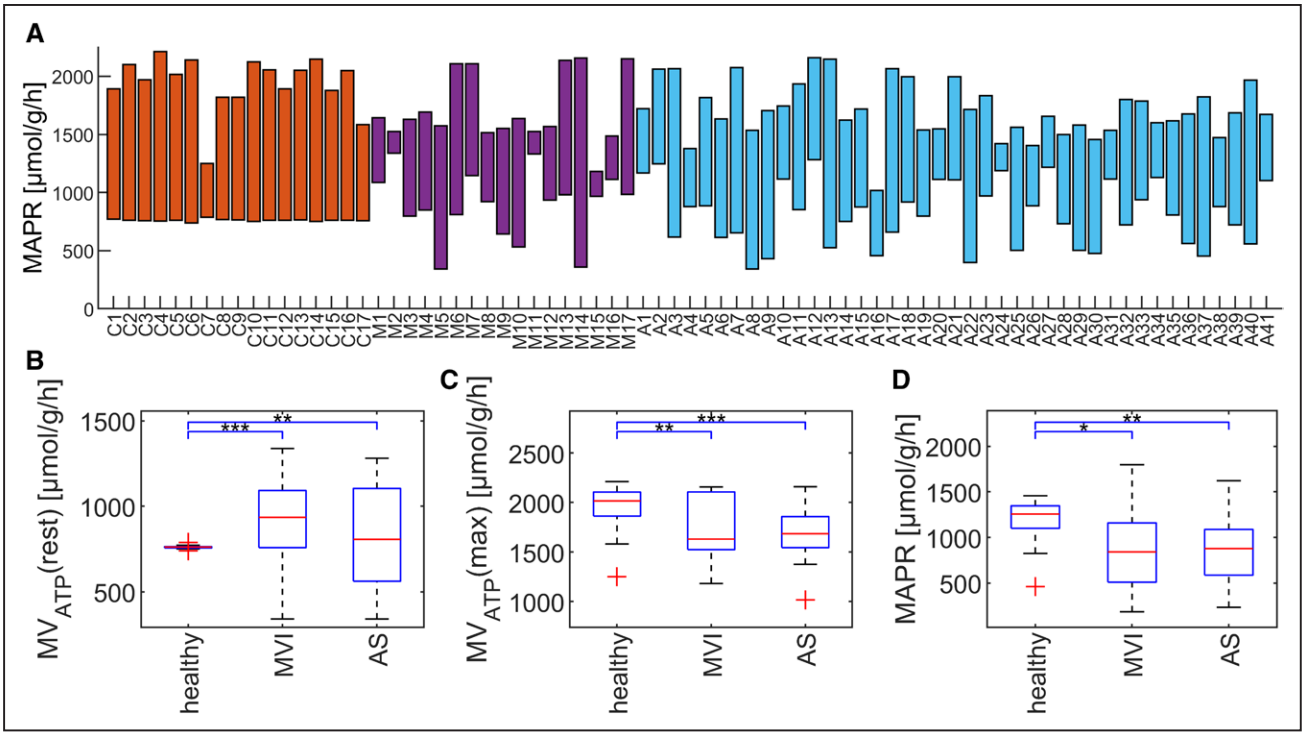

Figure 3. MV_{ATP}(rest) and MV_{ATP}(max) for controls and patients with mitral valve disease and aortic stenosis.
A, Bottom values of the bars refer to MV_{ATP}(rest); top values refer to MV_{ATP}(max). The bar length indicates the myocardial ATP production reserve (MAPR=MV_{ATP}[max] – MV_{ATP}[rest]). **B** through **D**, Box plots showing mean values, upper and lower quartiles, and total span of MV_{ATP}(rest), MV_{ATP}(max), and MAPR for controls and patients with mitral valve insufficiency (MVI) and aortic stenosis (AS). Significant differences between the patient groups are indicated by connecting brackets with asterisks giving the significance level (*P<0.05, **P<0.01, ***P<0.001). A Bonferroni correction was applied to account for multiple testing.

eter MV_{ATP}(rest) was significantly higher (890±292 vs 761±10 µmol/g/h), whereas MV_{ATP}(max) was significantly lower when compared with control values (1713±245 vs 1941±238 µmol/g/h; 2-sample Kolmogorov-Smirnov test). For patients with AS, the mean value of the parameter MV_{ATP}(rest) was also significantly higher (800±270 vs 761±10 µmol/g/h) and MV_{ATP}(max) was also significantly lower (1513±257 vs 1941±238 µmol/g/h). For both groups of patients, the parameter MAPR was on average significantly lower compared with the controls (826±448 in MVI and 904±340 in AS vs 1180±245 µmol/g/h). Hence, both groups of patients had on the average a reduced ATP production reserve, which was caused by increased MV_{ATP}(rest) and decreased MV_{ATP}(max).

Substrate Uptake of Patients at Rest and at Maximal Workload

Next, we investigated changes in the substrate preference of the LV accompanying altered metabolic capacity (Figure 4). In the resting state, the largest differences occurred for the uptake rates of glucose and lactate for patients with MVI. Glucose uptake was increased by >20%. At rest, there was a significant decrease in lactate utilization in patients with AS. In general, variances in substrate utilization rates were large, again pointing to individually differing metabolic phenotypes. The reduction in lactate utilization was significant also at maximal load in MVI and AS; glucose rates were significantly reduced only in patients with AS. Figure 4 also shows how the different substrates contribute to overall energy production. The contribution of fatty acids accounts for up to 2-thirds, whereas BCAAs always account for <1% of total energy expenditure and are therefore not shown.

Association of MV_{ATP} With Clinical Measures Evaluating the Mechanical Work and the Systolic Performance of the LV

In valve disease, the LV is exposed to chronic pressure load (AS) or volume overload (MVI). This results in a higher mechanical workload, which can be quantified by the surrogate internal myocardial power estimating the power of the LV required for cardiac contraction.[35] Our analysis provided evidence for a strong correlation between tMV_{ATP} at rest and at maximal pacing and the internal myocardial power (Figure 5). A significant correlation of the energy parameters has also been found with the cardiac output (Figure 5). Taken together, these findings demonstrate a close association between increased ATP production capacity, increased mechanical work of the pressure/volume overloaded LV, and cardiac output.

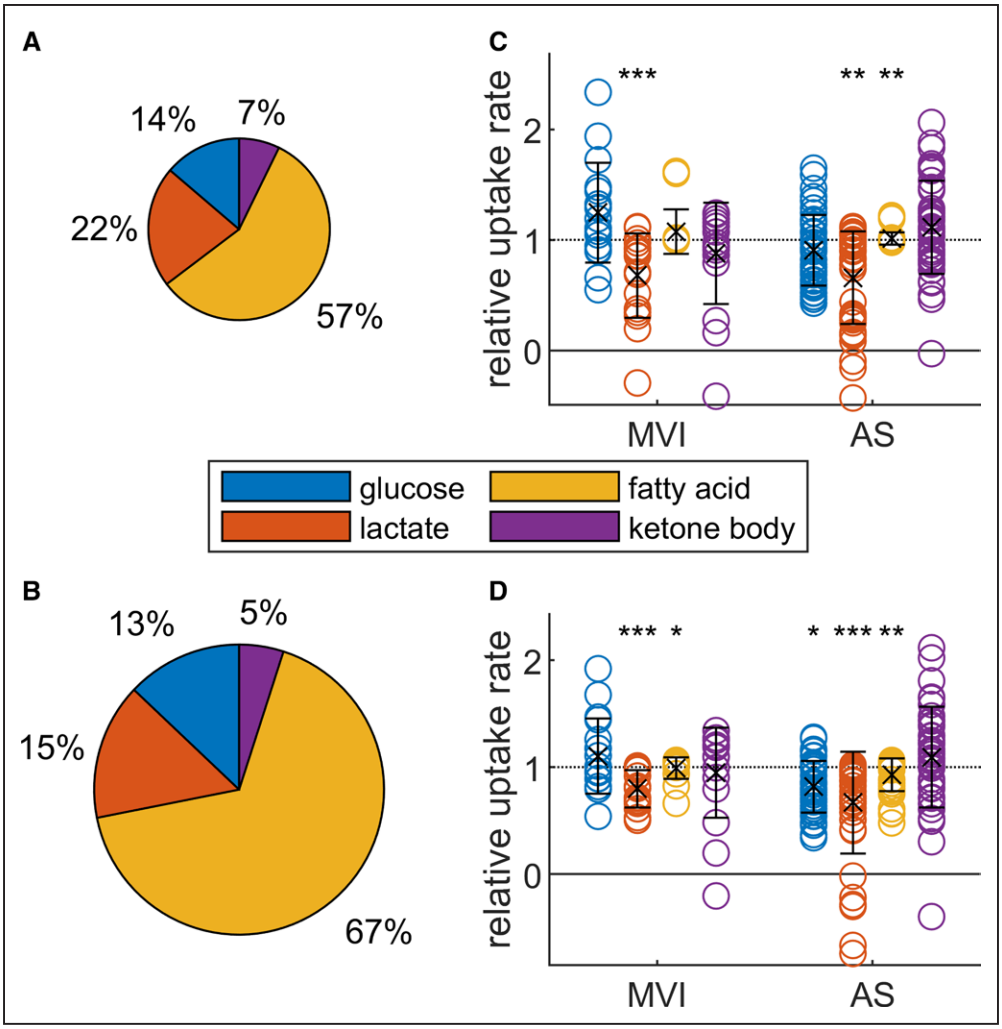

Figure 4. Contribution of energy-delivering substrates.
A and **B**, Relative contribution of the energy-delivering substrates to total energy expenditure at MV_{ATP}(rest) and MV_{ATP}(max) for the control group for 60 minutes pacing. Areas of the pie charts represent total energy expenditure. Changes of substrate uptake rates of patients with mitral valve insufficiency (MVI) or aortic stenosis (AS) relative to controls are shown at rest (**C**) and during maximal pacing (**D**). Plots show the relative change of substrate uptake rates of glucose (blue), lactate (orange), fatty acids (yellow), and ketone bodies (purple) for patients with MVI or AS during rest and at maximal ATP production rate after 60 minutes of pacing. Relative uptake rates are normalized to control values (ie, all control values are equal to 1). Significant changes from control are indicated by asterisks (*P<0.05, **P<0.01, ***P<0.001).

Metabolic Profiling of Individual Patients

Despite the general trend of the energy parameters in the patients' LV outlined in the preceding section, substantial differences in the metabolic profiles of individual patients occur. As an example, Figure 6 depicts the individual energetic profiles of 3 patients with AS with largely differing values of their cardiac energy parameters (Figure 3A). Patients A2 and A4 are characterized by impaired MAPR; patient A13 has a MAPR comparable to healthy hearts (Figure 3). The impaired MAPR of patient A2 results from an increased MV_{ATP}(rest) with a normal MV_{ATP}(max), whereas the impaired MAPR of patient A4 results from an increased MV_{ATP}(rest) and a decreased MV_{ATP}(max). Patient A13 with a normal MAPR has normal MV_{ATP}(rest) and normal MV_{ATP}(max). The individual alterations in the energetics of the LV are also associated with marked differences in substrate utilization rates. For example, whereas patient A13 has normal MV_{ATP}(rest), resting carbohydrate utilization rates (glucose and lactate) are strongly decreased and compensated by an increased KB utilization rate. This increased KB utilization is also maintained at MV_{ATP}(max) and is even more pronounced in patient A2. In contrast, patient A4 shows a decreased utilization rate for all substrates at MV_{ATP}(max).

Association of Preoperative Cardiac Metabolism With Postoperative Outcome

We also checked for a possible association between LV performance after valve surgery and the preoperative metabolic status of the LV. A univariate rank correlation analysis revealed a statistically significant association be-

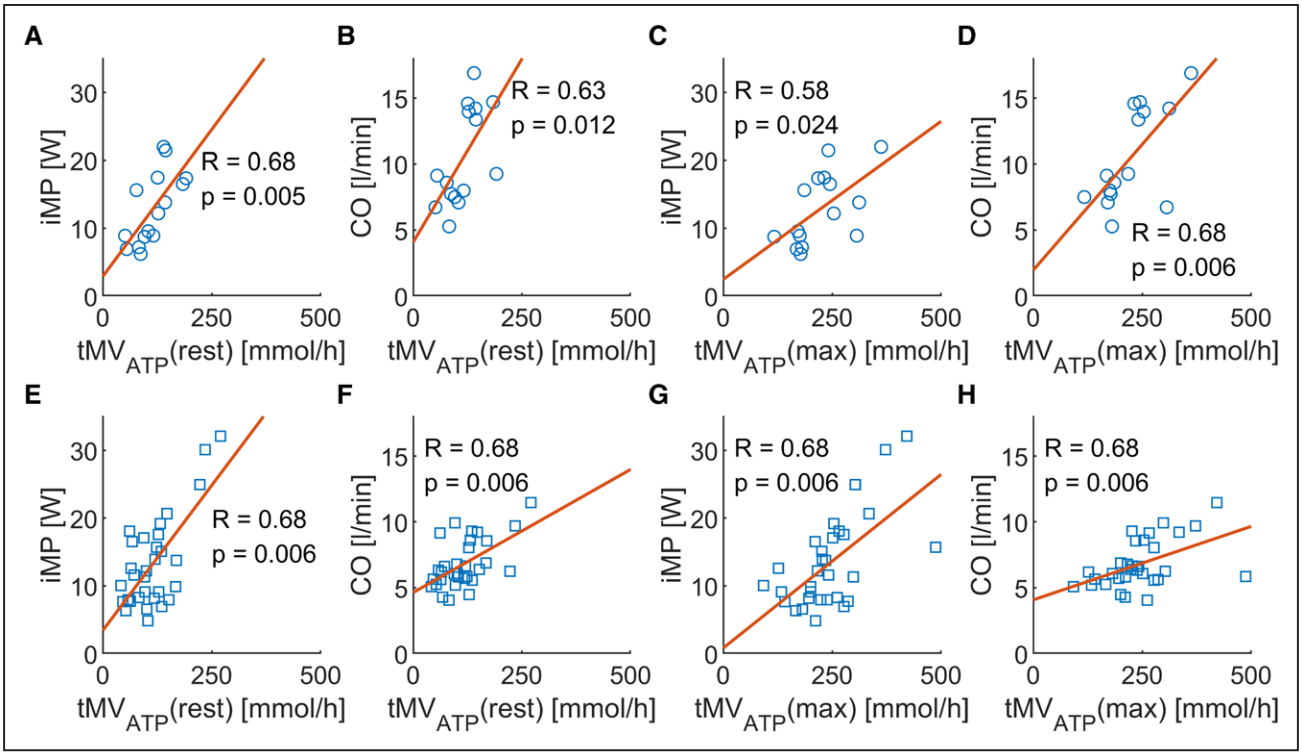

Figure 5. Correlation between tMV_{ATP}(rest) and tMV_{ATP}(max) and internal myocardial power as well as cardiac output for patients with mitral valve insufficiency or aortic stenosis.
A through **D,** Patients with mitral valve insufficiency (MVI). **E** through **H**, Patients with aortic stenosis (AS). iMP indicates internal myocardial power; and CO, cardiac output.

tween change in New York Heart Association (NYHA) functional classification (ΔNYHA = $NYHA_{postoperative}$ – $NYHA_{preoperative}$) and several metabolic capacities (Table S9), among them the maximal ATP production capacity in the postprandial state (P=0.02) and the maximal lactate uptake rate (P=0.01). This indicates that preoperative metabolic capability of the LV has an important effect on recovery and might be used as a prognostic marker in the future.

Statistical Analysis

For the patient characteristics in the Table, significance of parameter differences between AS and MVI groups was evaluated by means of 2-sided, 2-sample Wilcoxon-rank test in case of numeric data and χ^2 test with Yates continuity correction in case of categorical data.

Statistical significances between patient groups in Figure 3 and Figure 4 were evaluated by means of nonparametric Kolmogorov-Smirnov test. Statistical significance in Figure 3 was corrected for multiple testing by means of Bonferroni correction.

Correlations in Figure 5 are given as Pearson linear correlation coefficients with P values indicating statistical significance of the correlation computed by means of the Student t test.

Correlations between presurgery and postsurgery differences in NYHA Functional Classification and metabolic capacities (Table S9) were evaluated by calculation of Spearman rank correlation coefficients with P values indicating statistical significance of the correlation computed by means of the exact permutation test.

DISCUSSION

Novel Approach to Assess Myocardial ATP Producing Capacity

No method is available to measure MV_{ATP} in vivo. Invasive techniques, such as the determination of substrate extraction rates from coronary sinus, arterial concentration differences, or the oxidation rates of ^{14}C-labeled substrates from the rates of $^{14}CO_2$, have been applied in healthy people and patients with heart diseases.[36,37,46] However, such data cannot be directly converted into rates of ATP production. The same holds true for measurement of the myocardial oxygen consumption rate MVo_2 reflecting the overall myocardial oxidative metabolism. The MVo_2 does not capture the glycolytic ATP contribution, which is low under normoxic conditions but may increase 5-fold during development of heart failure[47] or even 20-fold during the transition from aerobic to anaerobic energy production.[48] Moreover, the ATP/O_2 ratio may change considerably with increasing workload owing to increasing cardiac preference for carbohydrates. This makes it difficult to convert O_2 consumption rates into ATP consumption rates. In addition, the maximal MVo_2 can be low because

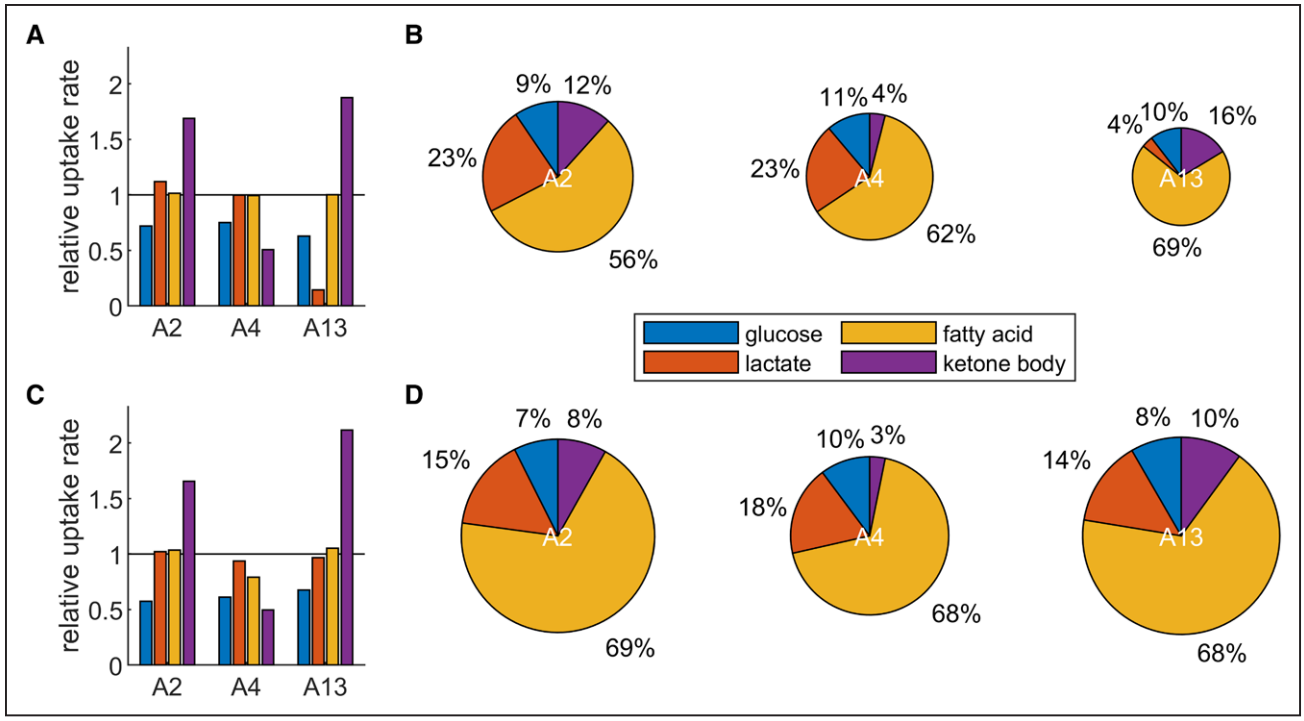

Figure 6. Metabolic characterization of 3 patients with aortic stenosis.
On the left, relative substrate utilization rates are shown compared with healthy controls at rest (**A**) and at maximal load (**C**). On the right, relative contribution of the different substrates (glucose [blue], lactate [orange], fatty acids [yellow], and ketone bodies [purple]) to overall ATP production rate at rest (**B**) and maximal load (**D**) are presented. Areas of pie diagrams represent total ATP production rate.

of restrictions imposed to heart performance by the nonmetabolic factors. To close this methodologic gap, we applied a novel approach to assess to energetic capacity of the LV of the human heart by combining kinetic modeling with protein abundance data of metabolic enzymes determined in cardiac tissue.

Reduced Myocardial Energetics in Patients With Valvular Disease

AS and MVI lead to chronic pressure or volume overload that result in phenotypically different myocardial remodeling (eccentric and concentric hypertrophy, respectively), both of which can progress to heart failure if left untreated. The cardiac adaptation processes to chronic overload conditions have been well characterized in terms of phenotyping and analysis of global cardiac function, but little is known about metabolic changes. The central findings of our approach are that even in patients with valvular dysfunction but preserved systolic function and no sign of heart failure, the energy metabolism is already deteriorated (Figure 3) and closely associated with mechanical power and systolic performance (Figure 5). The first finding is in line with several studies (reviewed in Sankaralingam and Lopaschuk),[49] which have established that a reduction in the ATP production capacity already occurs in early phases of heart failure development. The second finding identifies the capability of the cardiac metabolic network to generate ATP as the key link between systolic function and energy metabolism of the LV rather than the intracellular transport capacity of energy-rich phosphates by the creatine kinase shuttle, which was found to not be significantly different in patients with AS with preserved and reduced systolic function.[10]

MV_{ATP}(rest) was significantly increased in the MVI and AS groups and MV_{ATP}(max) was significantly decreased in both groups, resulting in a significant reduction of the specific ATP production reserve MAPR (Figure 3). The general decrease of MV_{ATP}(max) in both groups of patients can be accounted for by a decrease of the oxidative phosphorylation capacity as none of the investigated LVs showed excessive glycolytic activity. A decreased expression of the PGC-1α/PPARα transcription cascade has been identified as an important mechanism responsible for downregulation of the oxidative phosphorylation in the failing myocardium.[3]

Our analysis revealed in both groups of patients a large variability of the energy parameters (Figures 3 and 6), likely reflecting larger differences in the patient-specific functional and structural response of the LV to pressure/volume overload. Whereas some patients present with signs of hypertrophy, myocardial thickening, and ventricular dilation, others may show alterations in contraction time or only modest signs of remodeling.[50,51] It is in the nature of our approach that the large interindividual variabilities in the computed metabolic parameters are exclusively attributable to individual variabilities in the abundance of metabolic enzymes and transporters, and

these may be caused by individual differences in transcription, translation, or proteolysis. In a recent study, it was found that LV with normal aortic valves and with AS and aortic insufficiency disease all exhibit unique transcriptional profiles.[52] Thus, it appears more likely that the observed metabolic heterogeneity is caused by small RNA variabilities, including microRNAs and small transfer RNA fragments that can operate as modulators of the altered proteomics state.[53,54]

The large intraindividual variability of cardiac energetics in patients with valvular dysfunction necessitates an individual assessment of the metabolic status (Figure 6).

Our study revealed a significant correlation between improvement in NYHA staging after valve surgery and a substantial number of preoperative metabolic capacities. In line with this, Pasquet et al[55] identified cardiac glycolytic activity, assessed by means of 18-fluorodeoxyglucose positron emission tomography, as predictor of postoperative myocardial recovery after bypass surgery in patients with severe LV dysfunction. In principle, our approach allows inclusion of a large panel of metabolic capacities in the definition of novel risk predictors of postoperative outcome, but the additional benefit of such metabolic markers remains to be examined.

Alterations in the Myocardial Substrate Preference in Patients With Valvular Disease

Both groups of patients exhibited significant changes in myocardial use of the main energy substrates. There was a trend toward higher uptake rates for glucose and decreased uptake rates for lactate in patients with MVI and a decrease in glucose as well as lactate use in patients with AS. KB use rates showed high variability, but were generally increased in in patients with AS. This is in line with recent studies suggesting that increased reliance on KB metabolism offers a metabolic advantage in the failing heart and an ergogenic aid for exercise performance.[56,57]

Limitations of Our Approach

Our approach is restricted to the assessment of the energetic performance of an average cardiomyocyte working at fixed external concentrations of substrates and hormones. Hence, individual variances in circulating nutrients and hormones as well as activity-dependent concentration changes of oxygen and substrates attributable to changes of the coronary blood flow and the systemic metabolism (in particular skeletal muscle) were not taken into account. Moreover, it is well established that myocardial blood flow is heterogeneous on the local level and that this heterogeneity in perfusion entails heterogeneity in the metabolic endowment of cardiomyocytes.[58] For example, Bach et al.[59] demonstrated an association between heterogeneity of ventricular function and myocardial oxidative metabolism in nonischemic dilated cardiomyopathy. Thus, our analysis provides a comparison of metabolic capability under standardized conditions. The next step will be to incorporate the cellular metabolic model into a tissue-scale model of myocardial metabolism that includes local heterogeneity of blood flow, protein abundance, as well as individual plasma nutrient and hormone concentrations. Our previous work on liver metabolism[19,60,61] may serve as a paradigm for such a stepwise advancement of metabolic models from the cellular to the tissue level, but more in-depth data, such as histologic characterization and plasma metabolomics, will be required to enable such an approach.

Regarding the usefulness of our approach for the clinical assessment of heart diseases, the need for protein abundance data is the decisive limiting factor, because endomyocardial biopsies are most commonly used in surveillance of allograft rejection in patients who undergo heart transplant.

Conclusions

We investigated 2 different cohorts (AS and MVI) with large biophysical differences in terms of ventricular remodeling but comparable clinical state and ventricular function. Our approach can unravel differences in the energetic state of the myocardium even in hearts that have similar clinical markers of hypertrophy and pump function. The proposed model-based approach extends our capabilities to gain deeper insight into metabolic alterations in different types of heart diseases.

ARTICLE INFORMATION

Received May 18, 2021; accepted October 7, 2021.

Affiliations

Institute of Computer-Assisted Cardiovascular Medicine (N.B., J.E., I.W., S.N., M. Kelm, L.G., M.S., A.H., T.K.) and Institute of Biochemistry (J.E., I.W., H.-G.H.), Charité-Universitätsmedizin Berlin, corporate member of Freie Universität Berlin, and Humboldt-Universität zu Berlin, Germany. Department of Congenital Heart Disease–Pediatric Cardiology, Deutsches Herzzentrum Berlin (DHZB), Germany (S.N., M. Kelm, M.S., T.K.). Deutsches Zentrum für Herz-Kreislauf-Forschung eV (DZHK), Berlin, Germany (M. Kelm, T.G., T.K.). Berlin Institute of Health (BIH), Germany (M. Kelm, M. Kirchner, M.S., P.M.). Proteomics Platform, Max Delbrück Center for Molecular Medicine (MDC), Berlin, Germany (M. Kirchner, P.M.). Einstein Center Digital Future, Berlin, Germany (L.G.). Digital Health Center, Hasso Plattner Institute, University of Potsdam, Germany (M. Kraus). Department of Molecular Toxicology, German Institute of Human Nutrition Potsdam-Rehbruecke (DIfE), Nuthetal, Germany (T.G.).

Sources of Funding

This project was supported by the Deutsche Forschungsgemeinschaft (German Research Foundation; project 422215721) and by the Bundesministerium für Bildung und Forschung (German Federal Ministry of Education and Research) within the e:Med research program "SMART–Systems Medicine of Heart Failure" (grant 031A427A; URL: https://www.clinicaltrials.gov; Unique identifier: NCT03172338) as well as under the framework of ERA PerMed (HeartMed; grant 01KU2011A). This research was also funded by the European Research Area Network on Cardiovascular Diseases (SICVALVES). Drs Kelm and Schafstedde are participants in the BIH-Charité Digital Clinician Scientist Program funded by the Charité-Universitätsmedizin Berlin and the Berlin Institute of Health.

Disclosures

Patent application EP21174633, "Computer-assisted method for the evaluation of cardiac metabolism," was filed by Charité-Universitätsmedizin Berlin as employer of Dr Berndt and Prof Kuehne, with both holding inventorship for this patent application. The other authors report no conflicts.

Supplemental Material

Methods
Expanded Methods and Results S1–S3
Tables S1–S9
Figures S1–S10
References 62–119

REFERENCES

1. Evans RD, Clarke K. Myocardial substrate metabolism in heart disease. *Front Biosci (Schol Ed).* 2012;4:556–580. doi: 10.2741/285
2. Lopaschuk GD, Russell JC. Myocardial function and energy substrate metabolism in the insulin-resistant JCR:LA corpulent rat. *J Appl Physiol (1985).* 1991;71:1302–1308. doi: 10.1152/jappl.1991.71.4.1302
3. Neubauer S. The failing heart: an engine out of fuel. *N Engl J Med.* 2007;356:1140–1151. doi: 10.1056/NEJMra063052
4. Stanley WC, Recchia FA, Lopaschuk GD. Myocardial substrate metabolism in the normal and failing heart. *Physiol Rev.* 2005;85:1093–1129. doi: 10.1152/physrev.00006.2004
5. Taegtmeyer H, Young ME, Lopaschuk GD, Abel ED, Brunengraber H, Darley-Usmar V, Des Rosiers C, Gerszten R, Glatz JF, Griffin JL, et al; American Heart Association Council on Basic Cardiovascular Sciences. Assessing cardiac metabolism: a scientific statement from the American Heart Association. *Circ Res.* 2016;118:1659–1701. doi: 10.1161/RES.0000000000000097
6. Ingwall JS, Weiss RG. Is the failing heart energy starved? On using chemical energy to support cardiac function. *Circ Res.* 2004;95:135–145. doi: 10.1161/01.RES.0000137170.41939.d9
7. Herrmann G, Decherd Jr GM. The chemical nature of heart failure. *Ann Intern Med.* 1939;12:1233–1244.
8. Ning XH, Zhang J, Liu J, Ye Y, Chen SH, From AH, Bache RJ, Portman MA. Signaling and expression for mitochondrial membrane proteins during left ventricular remodeling and contractile failure after myocardial infarction. *J Am Coll Cardiol.* 2000;36:282–287. doi: 10.1016/s0735-1097(00)00689-6
9. Quigley AF, Kapsa RM, Esmore D, Hale G, Byrne E. Mitochondrial respiratory chain activity in idiopathic dilated cardiomyopathy. *J Card Fail.* 2000;6:47–55. doi: 10.1016/s1071-9164(00)00011-7
10. Peterzan MA, Clarke WT, Lygate CA, Lake HA, Lau JYC, Miller JJ, Johnson E, Rayner JJ, Hundertmark MJ, Sayeed R, et al. Cardiac energetics in patients with aortic stenosis and preserved versus reduced ejection fraction. *Circulation.* 2020;141:1971–1985. doi: 10.1161/CIRCULATIONAHA.119.043450
11. Abdurrachim D, Prompers JJ. Evaluation of cardiac energetics by non-invasive 31P magnetic resonance spectroscopy. *Biochim Biophys Acta Mol Basis Dis.* 2018;1864:1939–1948. doi: 10.1016/j.bbadis.2017.11.013
12. Ingwall JS. Phosphorus nuclear magnetic resonance spectroscopy of cardiac and skeletal muscles. *Am J Physiol.* 1982;242:H729–H744. doi: 10.1152/ajpheart.1982.242.5.H729
13. Peterzan MA, Lewis AJM, Neubauer S, Rider OJ. Non-invasive investigation of myocardial energetics in cardiac disease using 31P magnetic resonance spectroscopy. *Cardiovasc Diagn Ther.* 2020;10:625–635. doi: 10.21037/cdt-20-275
14. Karlstädt A, Fliegner D, Kararigas G, Ruderisch HS, Regitz-Zagrosek V, Holzhütter HG. CardioNet: a human metabolic network suited for the study of cardiomyocyte metabolism. *BMC Syst Biol.* 2012;6:114. doi: 10.1186/1752-0509-6-114
15. Cortassa S, Aon MA, Marbán E, Winslow RL, O'Rourke B. An integrated model of cardiac mitochondrial energy metabolism and calcium dynamics. *Biophys J.* 2003;84:2734–2755. doi: 10.1016/S0006-3495(03)75079-6
16. Beard DA. Modeling of oxygen transport and cellular energetics explains observations on in vivo cardiac energy metabolism. *PLoS Comput Biol.* 2006;2:e107. doi: 10.1371/journal.pcbi.0020107
17. Wu F, Yang F, Vinnakota KC, Beard DA. Computer modeling of mitochondrial tricarboxylic acid cycle, oxidative phosphorylation, metabolite transport, and electrophysiology. *J Biol Chem.* 2007;282:24525–24537. doi: 10.1074/jbc.M701024200
18. Wu F, Zhang EY, Zhang J, Bache RJ, Beard DA. Phosphate metabolite concentrations and ATP hydrolysis potential in normal and ischaemic hearts. *J Physiol.* 2008;586:4193–4208. doi: 10.1113/jphysiol.2008.154732
19. Berndt N, Bulik S, Wallach I, Wünsch T, König M, Stockmann M, Meierhofer D, Holzhütter HG. HEPATOKIN1 is a biochemistry-based model of liver metabolism for applications in medicine and pharmacology. *Nat Commun.* 2018;9:2386. doi: 10.1038/s41467-018-04720-9
20. Hughes CS, Moggridge S, Müller T, Sorensen PH, Morin GB, Krijgsveld J. Single-pot, solid-phase-enhanced sample preparation for proteomics experiments. *Nat Protoc.* 2019;14:68–85. doi: 10.1038/s41596-018-0082-x
21. Rappsilber J, Ishihama Y, Mann M. Stop and go extraction tips for matrix-assisted laser desorption/ionization, nanoelectrospray, and LC/MS sample pretreatment in proteomics. *Anal Chem.* 2003;75:663–670. doi: 10.1021/ac026117i
22. Tyanova S, Temu T, Cox J. The MaxQuant computational platform for mass spectrometry-based shotgun proteomics. *Nat Protoc.* 2016;11:2301–2319. doi: 10.1038/nprot.2016.136
23. Berndt N, Kann O, Holzhütter HG. Physiology-based kinetic modeling of neuronal energy metabolism unravels the molecular basis of NAD(P)H fluorescence transients. *J Cereb Blood Flow Metab.* 2015;35:1494–1506. doi: 10.1038/jcbfm.2015.70
24. Moors CC, van der Zijl NJ, Diamant M, Blaak EE, Goossens GH. Impaired insulin sensitivity is accompanied by disturbances in skeletal muscle fatty acid handling in subjects with impaired glucose metabolism. *Int J Obes (Lond).* 2012;36:709–717. doi: 10.1038/ijo.2011.123
25. Gordon RS Jr, Cherkes A. Unesterified fatty acid in human blood plasma. *J Clin Invest.* 1956;35:206–212. doi: 10.1172/JCI103265
26. Imaizumi A, Adachi Y, Kawaguchi T, Higasa K, Tabara Y, Sonomura K, Sato TA, Takahashi M, Mizukoshi T, Yoshida HO, et al. Genetic basis for plasma amino acid concentrations based on absolute quantification: a genome-wide association study in the Japanese population. *Eur J Hum Genet.* 2019;27:621–630. doi: 10.1038/s41431-018-0296-y
27. Nishioka M, Imaizumi A, Ando T, Tochikubo O. The overnight effect of dietary energy balance on postprandial plasma free amino acid (PFAA) profiles in Japanese adult men. *PLoS One.* 2013;8:e62929. doi: 10.1371/journal.pone.0062929
28. Ottosson F, Ericson U, Almgren P, Nilsson J, Magnusson M, Fernandez C, Melander O. Postprandial levels of branch chained and aromatic amino acids associate with fasting glycaemia. *J Amino Acids.* 2016;2016:8576730. doi: 10.1155/2016/8576730
29. Ravikumar B, Carey PE, Snaar JE, Deelchand DK, Cook DB, Neely RD, English PT, Firbank MJ, Morris PG, Taylor R. Real-time assessment of postprandial fat storage in liver and skeletal muscle in health and type 2 diabetes. *Am J Physiol Endocrinol Metab.* 2005;288:E789–E797. doi: 10.1152/ajpendo.00557.2004
30. Steinhauser ML, Olenchock BA, O'Keefe J, Lun M, Pierce KA, Lee H, Pantano L, Klibanski A, Shulman GI, Clish CB, et al. The circulating metabolome of human starvation. *JCI Insight.* 2018;3:121434. doi: 10.1172/jci.insight.121434
31. Bauer BA, Rogers PJ, Miller TD, Bove AA, Tyce GM. Exercise training produces changes in free and conjugated catecholamines. *Med Sci Sports Exerc.* 1989;21:558–562.
32. Dimsdale JE, Moss J. Plasma catecholamines in stress and exercise. *JAMA.* 1980;243:340–342.
33. Nelson RR, Gobel FL, Jorgensen CR, Wang K, Wang Y, Taylor HL. Hemodynamic predictors of myocardial oxygen consumption during static and dynamic exercise. *Circulation.* 1974;50:1179–1189. doi: 10.1161/01.cir.50.6.1179
34. Ritterhoff J, Tian R. Metabolism in cardiomyopathy: every substrate matters. *Cardiovasc Res.* 2017;113:411–421. doi: 10.1093/cvr/cvx017
35. Lee CB, Goubergrits L, Fernandes JF, Nordmeyer S, Knosalla C, Berger F, Falk V, Kuehne T, Kelm M. Surrogates for myocardial power and power efficiency in patients with aortic valve disease. *Sci Rep.* 2019;9:16407. doi: 10.1038/s41598-019-52909-9
36. Bergman BC, Tsvetkova T, Lowes B, Wolfel EE. Myocardial FFA metabolism during rest and atrial pacing in humans. *Am J Physiol Endocrinol Metab.* 2009;296:E358–E366. doi: 10.1152/ajpendo.90747.2008
37. Bergman BC, Tsvetkova T, Lowes B, Wolfel EE. Myocardial glucose and lactate metabolism during rest and atrial pacing in humans. *J Physiol.* 2009;587:2087–2099. doi: 10.1113/jphysiol.2008.168286
38. Bing RJ, Siegel A, Ungar I, Gilbert M. Metabolism of the human heart: II: studies on fat, ketone and amino acid metabolism. *Am J Med.* 1954;16:504–515. doi: 10.1016/0002-9343(54)90365-4
39. Camici P, Ferrannini E, Opie LH. Myocardial metabolism in ischemic heart disease: basic principles and application to imaging by positron

emission tomography. *Prog Cardiovasc Dis.* 1989;32:217–238. doi: 10.1016/0033-0620(89)90027-3
40. Gertz EW, Wisneski JA, Stanley WC, Neese RA. Myocardial substrate utilization during exercise in humans: dual carbon-labeled carbohydrate isotope experiments. *J Clin Invest.* 1988;82:2017–2025. doi: 10.1172/JCI113822
41. Mizuno Y, Harada E, Nakagawa H, Morikawa Y, Shono M, Kugimiya F, Yoshimura M, Yasue H. The diabetic heart utilizes ketone bodies as an energy source. *Metabolism.* 2017;77:65–72. doi: 10.1016/j.metabol.2017.08.005
42. Mudge GH Jr, Mills RM Jr, Taegtmeyer H, Gorlin R, Lesch M. Alterations of myocardial amino acid metabolism in chronic ischemic heart disease. *J Clin Invest.* 1976;58:1185–1192. doi: 10.1172/JCI108571
43. Voros G, Ector J, Garweg C, Droogne W, Van Cleemput J, Peersman N, Vermeersch P, Janssens S. Increased cardiac uptake of ketone bodies and free fatty acids in human heart failure and hypertrophic left ventricular remodeling. *Circ Heart Fail.* 2018;11:e004953. doi: 10.1161/CIRCHEARTFAILURE.118.004953
44. Nuutila P, Knuuti MJ, Raitakari M, Ruotsalainen U, Teräs M, Voipio-Pulkki LM, Haaparanta M, Solin O, Wegelius U, Yki-Järvinen H. Effect of antilipolysis on heart and skeletal muscle glucose uptake in overnight fasted humans. *Am J Physiol.* 1994;267:E941–E946. doi: 10.1152/ajpendo.1994.267.6.E941
45. Camici P, Marraccini P, Marzilli M, Lorenzoni R, Buzzigoli G, Puntoni R, Boni C, Bellina CR, Klassen GA, L'Abbate A. Coronary hemodynamics and myocardial metabolism during and after pacing stress in normal humans. *Am J Physiol.* 1989;257:E309–E317. doi: 10.1152/ajpendo.1989.257.3.E309
46. Kaijser L, Ericsson M, Walldius G. Fatty acid turnover in the ischaemic compared to the non-ischaemic human heart. *Mol Cell Biochem.* 1989;88:181–184. doi: 10.1007/BF00223441
47. Fillmore N, Levasseur JL, Fukushima A, Wagg CS, Wang W, Dyck JRB, Lopaschuk GD. Uncoupling of glycolysis from glucose oxidation accompanies the development of heart failure with preserved ejection fraction. *Mol Med.* 2018;24:3. doi: 10.1186/s10020-018-0005-x
48. Kübler W, Spieckermann PG. Regulation of glycolysis in the ischemic and the anoxic myocardium. *J Mol Cell Cardiol.* 1970;1:351–377. doi: 10.1016/0022-2828(70)90034-9
49. Sankaralingam S, Lopaschuk GD. Cardiac energy metabolic alterations in pressure overload-induced left and right heart failure (2013 Grover Conference Series). *Pulm Circ.* 2015;5:15–28. doi: 10.1086/679608
50. Dweck MR, Joshi S, Murigu T, Gulati A, Alpendurada F, Jabbour A, Maceira A, Roussin I, Northridge DB, Kilner PJ, et al. Left ventricular remodeling and hypertrophy in patients with aortic stenosis: insights from cardiovascular magnetic resonance. *J Cardiovasc Magn Reson.* 2012;14:50. doi: 10.1186/1532-429X-14-50
51. Enache R, Antonini-Canterin F, Piazza R, Popescu BA, Leiballi E, Marinigh R, Andriani C, Pecoraro R, Ginghina C, Nicolosi GL. CME: long-term outcome in asymptomatic patients with severe aortic regurgitation, normal left ventricular ejection fraction, and severe left ventricular dilatation. *Echocardiography.* 2010;27:915–922. doi: 10.1111/j.1540-8175.2010.01193.x
52. Greene CL, Jaatinen KJ, Wang H, Koyano TK, Bilbao MS, Woo YJ. Transcriptional profiling of normal, stenotic, and regurgitant human aortic valves. *Genes (Basel).* 2020;11:E789. doi: 10.3390/genes11070789
53. Mann DL. The emerging role of small non-coding RNAs in the failing heart: big hopes for small molecules. *Cardiovasc Drugs Ther.* 2011;25:149. doi: 10.1007/s10557-011-6292-x
54. Topkara VK, Mann DL. Role of microRNAs in cardiac remodeling and heart failure. *Cardiovasc Drugs Ther.* 2011;25:171–182. doi: 10.1007/s10557-011-6289-5
55. Pasquet A, Lauer MS, Williams MJ, Secknus MA, Lytle B, Marwick TH. Prediction of global left ventricular function after bypass surgery in patients with severe left ventricular dysfunction. Impact of pre-operative myocardial function, perfusion, and metabolism. *Eur Heart J.* 2000;21:125–136. doi: 10.1053/euhj.1999.1663
56. Aubert G, Martin OJ, Horton JL, Lai L, Vega RB, Leone TC, Koves T, Gardell SJ, Krüger M, Hoppel CL, et al. The failing heart relies on ketone bodies as a fuel. *Circulation.* 2016;133:698–705. doi: 10.1161/CIRCULATIONAHA.115.017355
57. Harvey KL, Holcomb LE, Kolwicz SC Jr. Ketogenic diets and exercise performance. *Nutrients.* 2019;11:E2296. doi: 10.3390/nu11102296
58. Deussen A, Lauer T, Loncar R, Kropp J. Heterogeneity of metabolic parameters in the left ventricular myocardium and its relation to local blood flow. *Basic Res Cardiol.* 2001;96:564–574. doi: 10.1007/s003950170008
59. Bach DS, Beanlands RS, Schwaiger M, Armstrong WF. Heterogeneity of ventricular function and myocardial oxidative metabolism in nonischemic dilated cardiomyopathy. *J Am Coll Cardiol.* 1995;25:1258–1262. doi: 10.1016/0735-1097(95)00019-Z
60. Berndt N, Holzhütter HG. Dynamic metabolic zonation of the hepatic glucose metabolism is accomplished by sinusoidal plasma gradients of nutrients and hormones. *Front Physiol.* 2018;9:1786. doi: 10.3389/fphys.2018.01786
61. Berndt N, Horger MS, Bulik S, Holzhütter HG. A multiscale modelling approach to assess the impact of metabolic zonation and microperfusion on the hepatic carbohydrate metabolism. *PLoS Comput Biol.* 2018;14:e1006005. doi: 10.1371/journal.pcbi.1006005
62. Ikeda Y, Okamura-Ikeda K, Tanaka K. Purification and characterization of short-chain, medium-chain, and long-chain acyl-CoA dehydrogenases from rat liver mitochondria: isolation of the holo- and apoenzymes and conversion of the apoenzyme to the holoenzyme. *J Biol Chem.* 1985;260:1311–1325.
63. Trumble GE, Smith MA, Winder WW. Purification and characterization of rat skeletal muscle acetyl-CoA carboxylase. *Eur J Biochem.* 1995;231:192–198. doi: 10.1111/j.1432-1033.1995.tb20686.x
64. Tucker GA, Dawson AP. The kinetics of rat liver and heart mitochondrial beta-hydroxybutyrate dehydrogenase. *Biochem J.* 1979;179:579–581. doi: 10.1042/bj1790579
65. Bulik S, Holzhütter HG, Berndt N. The relative importance of kinetic mechanisms and variable enzyme abundances for the regulation of hepatic glucose metabolism–insights from mathematical modeling. *BMC Biol.* 2016;14:15. doi: 10.1186/s12915-016-0237-6
66. Clutter WE, Bier DM, Shah SD, Cryer PE. Epinephrine plasma metabolic clearance rates and physiologic thresholds for metabolic and hemodynamic actions in man. *J Clin Invest.* 1980;66:94–101. doi: 10.1172/JCI109840
67. Sharma N, Okere IC, Brunengraber DZ, McElfresh TA, King KL, Sterk JP, Huang H, Chandler MP, Stanley WC. Regulation of pyruvate dehydrogenase activity and citric acid cycle intermediates during high cardiac power generation. *J Physiol.* 2005;562(Pt 2):593–603. doi: 10.1113/jphysiol.2004.075713
68. Saddik M, Gamble J, Witters LA, Lopaschuk GD. Acetyl-CoA carboxylase regulation of fatty acid oxidation in the heart. *J Biol Chem.* 1993;268:25836–25845.
69. Maoz D, Lee HJ, Deutsch J, Rapoport SI, Bazinet RP. Immediate no-flow ischemia decreases rat heart nonesterified fatty acid and increases acyl-CoA species concentrations. *Lipids.* 2005;40:1149–1154. doi: 10.1007/s11745-005-1479-9
70. Stanley WC, Meadows SR, Kivilo KM, Roth BA, Lopaschuk GD. Beta-Hydroxybutyrate inhibits myocardial fatty acid oxidation in vivo independent of changes in malonyl-CoA content. *Am J Physiol Heart Circ Physiol.* 2003;285:H1626–H1631. doi: 10.1152/ajpheart.00332.2003
71. Sun G, Yang K, Zhao Z, Guan S, Han X, Gross RW. Shotgun metabolomics approach for the analysis of negatively charged water-soluble cellular metabolites from mouse heart tissue. *Anal Chem.* 2007;79:6629–6640. doi: 10.1021/ac070843+
72. Bedi KC Jr, Snyder NW, Brandimarto J, Aziz M, Mesaros C, Worth AJ, Wang LL, Javaheri A, Blair IA, Margulies KB, et al. Evidence for intramyocardial disruption of lipid metabolism and increased myocardial ketone utilization in advanced human heart failure. *Circulation.* 2016;133:706–716. doi: 10.1161/CIRCULATIONAHA.115.017545
73. Idell-Wenger JA, Grotyohann LW, Neely JR. Coenzyme A and carnitine distribution in normal and ischemic hearts. *J Biol Chem.* 1978;253:4310–4318.
74. Russell RR III, Taegtmeyer H. Coenzyme A sequestration in rat hearts oxidizing ketone bodies. *J Clin Invest.* 1992;89:968–973. doi: 10.1172/JCI115679
75. Kalsi KK, Smolenski RT, Pritchard RD, Khaghani A, Seymour AM, Yacoub MH. Energetics and function of the failing human heart with dilated or hypertrophic cardiomyopathy. *Eur J Clin Invest.* 1999;29:469–477. doi: 10.1046/j.1365-2362.1999.00468.x
76. Kobayashi K, Neely JR. Control of maximum rates of glycolysis in rat cardiac muscle. *Circ Res.* 1979;44:166–175. doi: 10.1161/01.res.44.2.166
77. Wan B, Doumen C, Duszynski J, Salama G, Vary TC, LaNoue KF. Effects of cardiac work on electrical potential gradient across mitochondrial membrane in perfused rat hearts. *Am J Physiol.* 1993;265:H453–H460. doi: 10.1152/ajpheart.1993.265.2.H453
78. Chidsey CA, Weinbach EC, Pool PE, Morrow AG. Biochemical studies of energy production in the failing human heart. *J Clin Invest.* 1966;45:40–50. doi: 10.1172/JCI105322
79. Bowe C, Nzonzi J, Corsin A, Moravec J, Feuvray D. Lipid intermediates in chronically volume-overloaded rat hearts. Effect of diffuse ischemia. *Pflugers Arch.* 1984;402:317–320. doi: 10.1007/BF00585516
80. Masuda T, Dobson GP, Veech RL. The Gibbs-Donnan near-equilibrium system of heart. *J Biol Chem.* 1990;265:20321–20334.
81. Kashiwaya Y, Sato K, Tsuchiya N, Thomas S, Fell DA, Veech RL, Passonneau JV. Control of glucose utilization in working perfused rat heart. *J Biol Chem.* 1994;269:25502–25514.

82. Narabayashi H, Lawson JW, Uyeda K. Regulation of phosphofructokinase in perfused rat heart: requirement for fructose 2,6-bisphosphate and a covalent modification. *J Biol Chem.* 1985;260:9750–9758.
83. Kobayashi K, Neely JR. Mechanism of pyruvate dehydrogenase activation by increased cardiac work. *J Mol Cell Cardiol.* 1983;15:369–382. doi: 10.1016/0022-2828(83)90321-8
84. Wischeler BS, Müller-Ruchholtz ER, Reinauer H. [Influence of heart work and substrate uptake on the regulation of pyruvate dehydrogenase activity in isolated guinea pig hearts (author's transl).] *Pflugers Arch.* 1975;355:27–37. doi: 10.1007/BF00584797
85. El-Sharkawy AM, Gabr RE, Schär M, Weiss RG, Bottomley PA. Quantification of human high-energy phosphate metabolite concentrations at 3 T with partial volume and sensitivity corrections. *NMR Biomed.* 2013;26:1363–1371. doi: 10.1002/nbm.2961
86. Weiss RG, Gerstenblith G, Bottomley PA. ATP flux through creatine kinase in the normal, stressed, and failing human heart. *Proc Natl Acad Sci U S A.* 2005;102:808–813. doi: 10.1073/pnas.0408962102
87. Smith CS, Bottomley PA, Schulman SP, Gerstenblith G, Weiss RG. Altered creatine kinase adenosine triphosphate kinetics in failing hypertrophied human myocardium. *Circulation.* 2006;114:1151–1158. doi: 10.1161/CIRCULATIONAHA.106.613646
88. Bottomley PA, Wu KC, Gerstenblith G, Schulman SP, Steinberg A, Weiss RG. Reduced myocardial creatine kinase flux in human myocardial infarction: an in vivo phosphorus magnetic resonance spectroscopy study. *Circulation.* 2009;119:1918–1924. doi: 10.1161/CIRCULATIONAHA.108.823187
89. Meininger M, Landschütz W, Beer M, Seyfarth T, Horn M, Pabst T, Haase A, Hahn D, Neubauer S, von Kienlin M. Concentrations of human cardiac phosphorus metabolites determined by SLOOP 31P NMR spectroscopy. *Magn Reson Med.* 1999;41:657–663. doi: 10.1002/(sici)1522-2594(199904)41:4<657::aid-mrm3>3.0.co;2-i
90. Okada M, Mitsunami K, Inubushi T, Kinoshita M. Influence of aging or left ventricular hypertrophy on the human heart: contents of phosphorus metabolites measured by ^{31}P MRS. *Magn Reson Med.* 1998;39:772–782. doi: 10.1002/mrm.1910390515
91. Rovetto MJ, Lamberton WF, Neely JR. Mechanisms of glycolytic inhibition in ischemic rat hearts. *Circ Res.* 1975;37:742–751. doi: 10.1161/01.res.37.6.742
92. Cortassa S, Caceres V, Bell LN, O'Rourke B, Paolocci N, Aon MA. From metabolomics to fluxomics: a computational procedure to translate metabolite profiles into metabolic fluxes. *Biophys J.* 2015;108:163–172. doi: 10.1016/j.bpj.2014.11.1857
93. Randle PJ, England PJ, Denton RM. Control of the tricarboxylate cycle and its interactions with glycolysis during acetate utilization in rat heart. *Biochem J.* 1970;117:677–695. doi: 10.1042/bj1170677
94. Scharff R, Wool IG. Effect of diabetes on the concentration of amino acids in plasma and heart muscle of rats. *Biochem J.* 1966;99:173–178. doi: 10.1042/bj0990173
95. Morgan HE, Earl DC, Broadus A, Wolpert EB, Giger KE, Jefferson LS. Regulation of protein synthesis in heart muscle: I: effect of amino acid levels on protein synthesis. *J Biol Chem.* 1971;246:2152–2162.
96. Morgan HE, Chua BH, Fuller EO, Siehl D. Regulation of protein synthesis and degradation during in vitro cardiac work. *Am J Physiol.* 1980;238:E431–E442. doi: 10.1152/ajpendo.1980.238.5.E431
97. Whitmer JT, Idell-Wenger JA, Rovetto MJ, Neely JR. Control of fatty acid metabolism in ischemic and hypoxic hearts. *J Biol Chem.* 1978;253:4305–4309.
98. Cederbla G, Lindsted S, Lundholm K. Concentration of carnitine in human muscle-tissue. *Clin Chim Acta.* 1974;53:311-321. doi: 10.1016/0009-8981(74)90270-8
99. Denton RM, Randle PJ. Hormonal control of lipid concentration in rat heart and gastrocnemius. *Nature.* 1965;208:488. doi: 10.1038/208488a0
100. McGarry JD, Mills SE, Long CS, Foster DW. Observations on the affinity for carnitine, and malonyl-CoA sensitivity, of carnitine palmitoyltransferase I in animal and human tissues: demonstration of the presence of malonyl-CoA in non-hepatic tissues of the rat. *Biochem J.* 1983;214:21–28. doi: 10.1042/bj2140021
101. Minkler PE, Kerner J, Kasumov T, Parland W, Hoppel CL. Quantification of malonyl-coenzyme A in tissue specimens by high-performance liquid chromatography/mass spectrometry. *Anal Biochem.* 2006;352:24–32. doi: 10.1016/j.ab.2006.02.015
102. Reszko AE, Kasumov T, Comte B, Pierce BA, David F, Bederman IR, Deutsch J, Des Rosiers C, Brunengraber H. Assay of the concentration and 13C-isotopic enrichment of malonyl-coenzyme A by gas chromatography-mass spectrometry. *Anal Biochem.* 2001;298:69–75. doi: 10.1006/abio.2001.5349
103. Li Q, Sadhukhan S, Berthiaume JM, Ibarra RA, Tang H, Deng S, Hamilton E, Nagy LE, Tochtrop GP, Zhang GF. 4-Hydroxy-2(E)-nonenal (HNE) catabolism and formation of HNE adducts are modulated by β oxidation of fatty acids in the isolated rat heart. *Free Radic Biol Med.* 2013;58:35–44. doi: 10.1016/j.freeradbiomed.2013.01.005
104. Kasuya F, Oti Y, Tatsuki T, Igarashi K. Analysis of medium-chain acyl-coenzyme A esters in mouse tissues by liquid chromatography-electrospray ionization mass spectrometry. *Anal Biochem.* 2004;325:196–205. doi: 10.1016/j.ab.2003.10.043
105. la Fleur SE, Kalsbeek A, Wortel J, Fekkes ML, Buijs RM. A daily rhythm in glucose tolerance: a role for the suprachiasmatic nucleus. *Diabetes.* 2001;50:1237–1243. doi: 10.2337/diabetes.50.6.1237
106. Frangioudakis G, Gyte AC, Loxham SJ, Poucher SM. The intravenous glucose tolerance test in cannulated Wistar rats: a robust method for the in vivo assessment of glucose-stimulated insulin secretion. *J Pharmacol Toxicol Methods.* 2008;57:106–113. doi: 10.1016/j.vascn.2007.12.002
107. Hara E, Saito M. Diurnal changes in plasma glucose and insulin responses to oral glucose load in rats. *Am J Physiol.* 1980;238:E463–E466. doi: 10.1152/ajpendo.1980.238.5.E463
108. Stuenaes JT, Bolling A, Ingvaldsen A, Rommundstad C, Sudar E, Lin FC, Lai YC, Jensen J. Beta-adrenoceptor stimulation potentiates insulin-stimulated PKB phosphorylation in rat cardiomyocytes via cAMP and PKA. *Br J Pharmacol.* 2010;160:116–129. doi: 10.1111/j.1476-5381.2010.00677.x
109. Ramachandran C, Angelos KL, Walsh DA. Cyclic AMP-dependent and cyclic AMP-independent antagonism of insulin activation of cardiac glycogen synthase. *J Biol Chem.* 1982;257:1448–1457.
110. De Gasquet P, Griglio S, Pequignot-Planche E, Malewiak MI. Diurnal changes in plasma and liver lipids and lipoprotein lipase activity in heart and adipose tissue in rats fed a high and low fat diet. *J Nutr.* 1977;107:199–212. doi: 10.1093/jn/107.2.199
111. Yamamoto H, Nagai K, Nakagawa H. Role of SCN in daily rhythms of plasma glucose, FFA, insulin and glucagon. *Chronobiol Int.* 1987;4:483–491. doi: 10.3109/07420528709078539
112. Djordjevic J, Jasnic N, Vujovic P, Djurasevic S, Djordjevic I, Cvijic G. The effect of fasting on the diurnal rhythm of rat ACTH and corticosterone secretion. *Arch Biol Sci.* 2008;60:541–546. doi: 10.2298/ABS0804541D
113. Clark MG, Patten GS. Adrenergic regulation of glucose metabolism in rat heart: a calcium-dependent mechanism mediated by both alpha- and beta-adrenergic receptors. *J Biol Chem.* 1984;259:15204–15211.
114. Henderson MJ, Morgan HE, Park CR. Regulation of glucose uptake in muscle: V: the effect of growth hormone on glucose transport in the isolated, perfused rat heart. *J Biol Chem.* 1961;236:2157–2161.
115. Morgan HE, Henderson MJ, Regen DM, Park CR. Regulation of glucose uptake in muscle: I: the effects of insulin and anoxia on glucose transport and phosphorylation in the isolated, perfused heart of normal rats. *J Biol Chem.* 1961;236:253–261.
116. Drake AJ, Haines JR, Noble MI. Preferential uptake of lactate by the normal myocardium in dogs. *Cardiovasc Res.* 1980;14:65–72. doi: 10.1093/cvr/14.2.65
117. Vyska K, Meyer W, Stremmel W, Notohamiprodjo G, Minami K, Machulla HJ, Gleichmann U, Meyer H, Körfer R. Fatty acid uptake in normal human myocardium. *Circ Res.* 1991;69:857–870. doi: 10.1161/01.res.69.3.857
118. Stremmel W. Fatty acid uptake by isolated rat heart myocytes represents a carrier-mediated transport process. *J Clin Invest.* 1988;81:844–852. doi: 10.1172/JCI113393
119. Sultan AM. Effects of diabetes and insulin on ketone bodies metabolism in heart. *Mol Cell Biochem.* 1992;110:17–23. doi: 10.1007/BF02385001